

$B \rightarrow J/\psi X$ in the Inclusive Parton and the ACCMM Model *

William F. Palmer

Department of Physics, The Ohio State University
Columbus, OH 43210, USA

Emmanuel A. Paschos, Peter H. Soldan
Institut für Physik, Universität Dortmund
D-44221 Dortmund, Germany

February 22, 1996

Abstract

The parton model as developed for semileptonic B decays is applied to the inclusive decay $B \rightarrow J/\psi X$. We calculate the momentum spectrum of the J/ψ using a one-parameter distribution function for the heavy quark, taken from production experiments, and compare our results with recent data from CLEO which fixes the distribution parameter ε_p . An analogous calculation is carried out in the ACCMM model where the data determines the Fermi motion parameter p_f .

The models give a good description of the data, provided in each of them the parameter in the distribution function is chosen to correspond to a softer b quark momentum distribution than that commonly used in studies of semileptonic B decays. In particular we arrive at $\varepsilon_p = \mathcal{O}(0.008)$ and $p_f = \mathcal{O}(0.55 \text{ GeV})$, respectively. The latter value ($p_f = 0.5 \text{ GeV}$) produces in the ACCMM model $10^2 \times |V_{ub}/V_{cb}|^2 = 1.03$, which removes a former supposed discrepancy with the ISGW model. Finally, the strength of the effective color singlet coefficient is found to be $|a_2| = \mathcal{O}(0.28)$ in both models.

*This work was supported in part by the Bundesministerium für Forschung und Technologie, 056DO93P(5), Bonn, FRG, by the CEC Science Project n° SC1-CT91-0729, and by the US Department of Energy under grant DOE/ER/01545-605

1 Introduction

The distribution of charmonium states in B meson decays is of special interest, because it provides a testing ground for color suppression in B decays already attainable in the present experiments. At the b mass scale, a leading order calculation generates a consistent pattern of color suppression for the production of S -wave charmonium states. In the context of the ‘color singlet mechanism’ the production is related to the decay of a b quark in the B meson, at short distances, into a color singlet $c\bar{c}$ pair plus other quarks and gluons. The c and \bar{c} have almost equal momenta and reside in the appropriate angular-momentum state. This subprocess is dominated by the color suppressed internal W -exchange diagram, where hard gluon exchanges lead to an effective neutral current [1]. Deviations from this leading order ‘singlet mechanism’, which arise from relativistic corrections and soft gluon induced fragmentation of the $c\bar{c}$ into charmonium, affect the normalization but not the structure of the amplitude $b \rightarrow J/\psi X$ (in which X sums over hadronic states) [2].

Several authors made predictions for the branching ratio of the direct decay $b \rightarrow J/\psi X$ to leading order in α_s [1–5]. Recently a next-to-leading order QCD calculation was reported [6]. The authors pointed out that the process under consideration cannot be explained presently by a standard application of perturbative QCD. The difficulties entering the analysis arise from the strong suppression of the leading order color singlet Wilson coefficient, causing considerable cancellations in three different orders of α_s . Alternatively one may use a phenomenological factorization approach and take into account deviations from this prescription by replacing the color singlet renormalization coefficient by an effective neutral current coefficient a_2 , which has to be determined from experimental data in a model dependent way.

Both ARGUS and CLEO reported on inclusive B decays to J/ψ , where they identified a sizable component of decays with three or more particles in the final state [7, 8]. In a recent publication [9] CLEO presented an analysis based on a data sample, which is one order of magnitude larger than those of previous studies, corresponding to an error reduction by a factor of 2.4. A comparison between theory and experiment requires the branching ratio resulting from *direct* decays. Therefore the group corrected the measured J/ψ spectrum for the ‘feed-down’ modes $B \rightarrow \psi(2s) X$ and $B \rightarrow \chi_{c1} X$. As a result they found the direct branching ratio $(0.80 \pm 0.08)\%$. A theoretical analysis carried out by the CLEO group following Ref. [1] yields 0.75%, in good agreement with the measurement, where the phenomenological factorization prescription has been applied using a value $|a_2| = 0.23$.

The latter value has to be modified when incorporating bound state effects for the initial B meson, which have to be included in order to gain a theoretical prediction of the J/ψ

momentum spectrum within an inclusive approach. So far there is not available a detailed fit to experimental data of momentum spectra obtained from theory. Palmer and Stech have made a preliminary attempt using a simple wave function formalism [10]. In this paper we will investigate two different approaches in order to account for the experimental results.

As stated above a sizable component of the momentum spectrum is due to nonresonant multi-particle final states. Consequently, for a wide range of phase-space an inclusive description using quark-hadron duality, which was extensively applied in the inclusive *semileptonic* decays of B mesons, will be appropriate.

The semileptonic decays involve large energies and momentum transfers of the weak current over most of the phase-space. Several groups noticed that these kinematic regions investigate the light-cone behaviour of currents for which the methods of deep inelastic scattering are valid. There are various approaches available which derived useful results describing the lepton spectrum in the decay $B \rightarrow X_{u(c)} e \nu$. These approaches use different formalisms, but they still follow two basic steps.

(i) The decay of the $b \rightarrow u(c)$ which are propagating as free particles is considered and the resulting spectrum is folded with the momentum distribution of the b quark obtaining moments of the quark distribution [11, 12]. A similar approach is given by the ACCMM model [16], in which one accounts for the binding effects by treating the spectator quark as particle on the mass shell with nonzero momentum and averages over this momentum.

(ii) After the introduction of the point-like behaviour one still has to calculate the expectation value of the bilocal transition operator between the initial hadronic state to gain the width of the decay. In this context the new development is the application of the operator product expansion (OPE), which involves an expansion in inverse powers of the heavy quark mass m_b incorporating the formalism of the Heavy Quark Effective Theory (HQET) [17]. The calculation of the lepton energy spectra requires a modified expansion in powers of $1/(1-y)m_b$ with y being the normalized lepton energy [18–23].

The analytic form of the structure function of the heavy quark within the B meson controls the endpoint behaviour of the leptonic spectrum, since in this region the OPE does not converge. It has been shown that the prediction of HQET far from the endpoint gives approximately the same shape of the spectrum as the ACCMM model with a Fermi motion parameter $p_f \simeq 0.3$ GeV [24]. Yet the model dependence of this region is quite small [25]. Therefore it is of great relevance to test the approaches with decay channels of the B meson different from the semileptonic one in order to extract the momentum distribution

function of the heavy quark in a direct way and then compare it with the distribution function obtained in semileptonic decays.

The inclusive decay $B \rightarrow J/\psi X$ provides a well suited testing ground since, as we shall show, in this process the dependence on the structure function of the b quark is more direct, i.e., the J/ψ momentum spectrum is proportional to the distribution function.

A QCD based analysis of the decay using HQET is only of limited validity, since due to the smaller energy release the convergence of the OPE is less reliable than for semileptonic decays. Therefore one has to resort to a formalism in which the structure function can be modeled in terms of parameters that may be obtained from experiment. We will apply two different approaches. In Section 2 we present a field-theoretical version of the inclusive parton model, which two of us together with Jin already applied for semileptonic decays [11, 12]. In Section 3 we calculate the J/ψ momentum spectrum within the framework of the ACCMM model. In each of the analyses we determine the distribution parameter of the structure function from a comparison to the recent CLEO data. The overall normalization of the theoretical spectra further provides information respecting the value of the effective color singlet coefficient $|a_2|$. Finally we use our results to extract the value of $|V_{ub}/V_{cb}|$ in the ACCMM model from the semileptonic decay channel of the B . This procedure requires some additional remarks which are given in Section 4. In Section 5 we compare our results with experimental data for the polarization of the J/ψ . The summary can be found in Section 6.

2 $B \rightarrow J/\psi X$ in the Inclusive Parton Model (IPM)

2.1 Calculation of the Differential Branching Ratio

In order to investigate the interaction which induces charmonium production in B decays, we start at the quark level at a high-energy scale where the Hamiltonian is known. This is renormalized to lower energies to produce an effective four-fermion interaction

$$\mathcal{H}_{eff} = \frac{G_F}{\sqrt{2}} V_{cb} V_{cs}^* \left[\left(c_2 + \frac{1}{3} c_1 \right) \bar{s} \gamma_\mu^L b \bar{c} \gamma_\mu^L c + \frac{1}{2} c_1 \bar{c} \gamma_\mu^L \lambda^i c \bar{s} \gamma_\mu^L \lambda^i b \right] + \{s \rightarrow d\}, \quad (1)$$

$\gamma_\mu^L = \gamma_\mu(1 - \gamma_5)$, where operators arising from penguin and box diagrams have been neglected. The first term is a color singlet, the second a color octet operator. The renormalization functions (Wilson coefficients) $c_i(\mu)$ have been computed up to the next-to-leading order corrections in Ref. [26].

The effective interaction (1) is evaluated using a factorization prescription by which the amplitude can be written as a product of matrix elements of current operators. Deviations

from this prescription are parametrized by substituting the color suppressed singlet coefficient by a free parameter a_2 which is written in terms of the effective number of colors ($1/\xi$) and has to be determined by model-dependent fits to the experimental data,

$$\left(c_2 + \frac{1}{N_c}c_1\right) \rightarrow a_2 = c_2 + \xi c_1. \quad (2)$$

a_2 is equivalent to the coefficient introduced for type-II processes in the factorization model of BSW [27] for *exclusive* decays. Using CLEO data from two-body decay modes with J/ψ mesons in the final state, an analysis within the BSW model yields [28]

$$|a_2| = 0.26 \pm 0.01 \pm 0.01 \pm 0.02, \quad (3)$$

where the second systematic error is due to the B meson production fractions and lifetimes. Theoretical uncertainties mainly due to hadronic form factors are not included. A corresponding analysis [29] using the model of *Neubert et al.* [30] provides a central value $|a_2| = 0.23$, whereas that of *Deandrea et al.* [31] yields $|a_2| = 0.25$ (for $|V_{cb}| = 0.041$, $\tau_B = 1.44$ ps and $f_{D(D^*)} = 220$ MeV).

In this paper we extend the factorization model for exclusive two-body decays to an inclusive picture at the quark level. This is reasonable because, as was stated in Ref. [32], many-body final states will most likely start as two color singlet quark antiquark pairs, including intermediate massive resonances, where strong phases from final state interactions disappear in the sum of all states. The authors of Ref. [32] made use of this inclusive picture to determine the lifetime ratio $\tau(B^+)/\tau(B^0)$. As we intend to reproduce not only the branching ratio but also the momentum spectrum for the decay $B \rightarrow J/\psi X$, we have to incorporate the momentum distribution of the b quark in the B meson. In our analysis we will let the effective color singlet coefficient $|a_2|$ to float within the range which is covered by the various models for exclusive modes.

We consider the matrix element of the Hamiltonian (1) for our process (in the explicit notation we only refer to the dominant decay involving an s quark in the final state),

$$\langle J/\psi X_s | \mathcal{H}_{eff} | B \rangle = a_2 \frac{G_f}{\sqrt{2}} V_{cb} V_{cs}^* \langle J/\psi | \bar{c} \gamma_\mu^L c | 0 \rangle \langle X_s | \bar{s} \gamma_L^\mu b | B \rangle, \quad (4)$$

where we make use of the phenomenological factorization prescription. The second term of Eq. (1) does not contribute between color singlet states.

For the matrix element of the $\bar{c}c(1S)$ at the origin we use the current-identity for pure vector-like states,

$$\langle 0 | \bar{c}(0) \gamma_\mu^L c(0) | J/\psi \rangle = \varepsilon_\mu f_\psi M_\psi. \quad (5)$$

This identification is valid, because the time-scale of the interaction to be considered is larger than the scale for the formation of the singlet state ($t_{int} > 1/M_\psi$). f_ψ is the J/ψ decay constant and can, to leading order in the relative heavy quark velocity v , be related to the radial part of its nonrelativistic wave function. In principle one can determine f_ψ from the electromagnetic decay $J/\psi \rightarrow e^+e^-$, but practically one is confronted with the ignorance of higher order QCD corrections to the decay rate which might be of great relevance in view of existing large leading order corrections. Within the studies of *exclusive* two-body decays $B \rightarrow J/\psi M$ [30] the central value of the decay constant was fixed at $f_\psi = 0.384$ GeV which results from the omission of any QCD correction (as of relativistic corrections to the wave function of the J/ψ). This analysis refers to the 1990 Particle Data Group value for the branching ratio of $J/\psi \rightarrow e^+e^-$. Therefore when extracting $|a_2|$ from *inclusive* B decays we will use the above value in order to compare the result with Eq. (3). This procedure requires some additional remarks which concern both the studies of exclusive and inclusive decays.

Relating the parameter which contains the nonperturbative effects in the production of $1S$ -charmonium with the J/ψ decay constant implies the neglect of color octet contributions to the fragmentation process in the explicit calculation. In Ref. [2] it was argued in the framework of nonrelativistic QCD (NRQCD), that the fragmentation of a $(\bar{c}c)_8(^3S_1)$ state into a J/ψ in the long-distance scale may give sizable contributions to the $B \rightarrow J/\psi X$ decay rate. This feature occurs, despite the fact that the color octet operator is of the order $\mathcal{O}(v^4)$ respecting the velocity counting rules in the NRQCD, because of the large suppression of the color singlet Wilson coefficient.

As the structure of the amplitude for the effective point-like decay $b \rightarrow J/\psi X$ remains unchanged, considering nonleading effects in the fragmentation process only affects the normalization of the $B \rightarrow J/\psi X$ decay spectrum. Using the leading order value $f_\psi = 0.384$ GeV therefore means that the effective neutral current coefficient $|a_2|$, which is determined from a comparison with experimental data, includes contributions due to the charmonium fragmentation. Consequently, since these contributions are different for various charmonium states [2], the universality of $|a_2|$ is limited to B decays involving fixed S -wave resonances.

Reducing the matrix element (4) of the mesonic decay $B \rightarrow J/\psi X_s$ to that of the point-like effective neutral current subprocess $b \rightarrow J/\psi s$ (see Fig. 1c) in the valence quark approximation one obtains

$$\langle J/\psi X_s | \mathcal{H}_{eff} | B \rangle = a_2 V_{cb} V_{cs}^* M_\psi f_\psi \frac{G_F}{\sqrt{2}} \varepsilon_\mu^* \bar{s} \gamma^\mu (1 - \gamma_5) b. \quad (6)$$

This expression for a free quark decay has to be modified by incorporating bound state corrections due to the strong interaction between heavy and light quark in the initial meson. In the *intuitive* parton model one has to take the incoherent sum over all subprocesses in which a distribution function $f(x)$ is introduced as a weight,

$$\Gamma_B = \int_0^1 dx f(x) \Gamma_b(x), \quad \text{where} \quad \int_0^1 f(x) dx = 1. \quad (7)$$

In Eq. (7) transverse momenta of the heavy quark relative to the B meson are neglected which leads to the Lorentz invariant prescription $p_b^\mu = xP_B^\mu$. This approach corresponds to an equal velocity approximation, i.e., valence quarks and B meson have the same velocity, and is valid at the infinite momentum frame. We therefore proceed as usual computing a Lorentz invariant quantity and then use it in any other frame.

The basis for our approach is given by a *field-theoretical* version of the parton model. If we square the second matrix element on the right-hand side of Eq. (4) and sum over all final states, which guarantees incoherence, we produce the hadronic tensor corresponding to the effective transition $B \rightarrow X_f$,

$$W_{\mu\nu} = -\frac{1}{2\pi} \int d^4y e^{iqy} \langle B | [j_\mu(y), j_\nu^\dagger(0)] | B \rangle, \quad (8)$$

where $j_\mu(x) = : \bar{q}_f \gamma_\mu^L b(x) :$ is the left-handed effective neutral current. The same tensor structure we encountered in the semileptonic B meson decays [11–14]. Substituting for the leptonic tensor the corresponding expression of the J/ψ current,

$$L_{\mu\nu}(J/\psi) = 2\pi^3 |V_{cf}|^2 |a_2|^2 f_\psi^2 M_\psi^2 \left(-g_{\mu\nu} + \frac{(k_\psi)_\mu (k_\psi)_\nu}{M_\psi^2} \right), \quad (9)$$

we can write the differential rate for the decay $B \rightarrow X_f J/\psi$ in the restframe of the B in exact analogy to the semileptonic decay,

$$d\Gamma_{(B \rightarrow X_f J/\psi)} = \frac{G_F^2 |V_{cb}|^2}{(2\pi)^5 M_B} L_{\mu\nu} W^{\mu\nu} \frac{d^3 k_\psi}{2E_\psi}. \quad (10)$$

The general structure of the hadronic tensor reads

$$\begin{aligned} W^{\mu\nu} = & -g^{\mu\nu} W_1 + \frac{1}{M_B^2} P_B^\mu P_B^\nu W_2 - i\varepsilon^{\mu\nu\alpha\beta} \frac{1}{M_B^2} P_{B\alpha} q_\beta W_3 \\ & + \frac{1}{M_B^2} q^\mu q^\nu W_4 + \frac{1}{M_B^2} (P_B^\mu q^\nu + P_B^\nu q^\mu) W_5 + \frac{1}{M_B^2} i(P_B^\mu q^\nu - P_B^\nu q^\mu) W_6, \end{aligned} \quad (11)$$

where in our case $q = k_\psi$. Introducing the light-cone dominance as in Ref. [11–15] allows to refer the tensor corresponding to the transition $B \rightarrow X_f$ in the decay $B \rightarrow X_f J/\psi$ to the distribution function $f(x)$ of the heavy quark momentum,

$$W_{\mu\nu,f} = 4(S_{\mu\rho\nu\lambda} - i\varepsilon_{\mu\rho\nu\lambda}) \int dx f(x) P_B^\lambda (xP_B - k_\psi)^\rho \varepsilon[(xP_B - k_\psi)_0] \delta[(xP_B - k_\psi)^2 - m_f^2], \quad (12)$$

with

$$S_{\mu\rho\nu\lambda} = g_{\mu\rho}g_{\nu\lambda} - g_{\mu\nu}g_{\rho\lambda} + g_{\mu\lambda}g_{\nu\rho} \quad \text{and} \quad \varepsilon(x) = \begin{cases} +1, & x > 0 \\ -1, & x < 0. \end{cases} \quad (13)$$

From Eqs. (11) and (12) one obtains the structure functions W_i of the hadronic tensor in the restframe of the B meson, which two of us together with Jin derived in Ref. [11, 12] in exact analogy for the semileptonic decay rate,

$$\begin{aligned} W_1 &= 2[f(x_+) + f(x_-)], & W_2 &= \frac{8}{x_+ - x_-} [x_+ f(x_+) - x_- f(x_-)], \\ W_3 = W_5 &= \frac{-4}{x_+ - x_-} [f(x_+) - f(x_-)], & W_4 = W_6 &= 0, \end{aligned} \quad (14)$$

where we have defined

$$M_B x_{\pm} = \frac{1}{M_B} \left(P_B k_{\psi} \pm \sqrt{(P_B k_{\psi})^2 + (m_f^2 - M_{\psi}^2) M_B^2} \right) \big|_{|\vec{p}_B|=0} \left(E_{\psi} \pm \sqrt{|\vec{k}_{\psi}|^2 + m_f^2} \right). \quad (15)$$

For the case of a massless final state quark x_{\pm} are identical to the usual light-cone variables. The dependence of the distribution function on the single scaling variable x is a consequence of the light-cone dominance, since in this framework the structure function $f(x)$ is obtained as the Fourier transform of the reduced bilocal matrix element, which contains the long-distance contributions to the hadronic tensor [13],

$$f(x) = \int d(y P_B) e^{ix(y P_B)} \frac{1}{4\pi M_B^2} \langle B | \bar{b}(0) P_B^{\mu} \gamma_{\mu}^L b(y) | B \rangle \big|_{y^2=0}. \quad (16)$$

The terms proportional to $f(x_-)$ in Eq. (14) are a result of the field-theoretical approach. The kinematical range for x_- belongs to a final state quark with negative energy. Therefore the corresponding terms can be associated, formally, with quark pair-creation in the B meson (see Fig. 1b), whereas the dominant terms proportional to $f(x_+)$ reflect the direct decay of Fig. 1a.

Including the small $f(x_-)$ term as well as the CKM-suppressed transition $c \rightarrow d$ the Lorentz invariant width of the decay $B \rightarrow J/\psi X$ reads

$$\begin{aligned} E_B \cdot d\Gamma_{(B \rightarrow J/\psi X)} &= \sum_{f=s,d} \frac{|C_f|^2}{2\pi^2} \int dx f(x) \left[P_B(x P_B - k_{\psi}) + \frac{2}{M_{\psi}^2} (P_B k_{\psi})(x P_B k_{\psi} - M_{\psi}^2) \right] \\ &\quad \times \varepsilon[(x P_B - k_{\psi})_0] \delta^{(1)} \left[(x P_B - k_{\psi})^2 - m_f^2 \right] \frac{d^3 k_{\psi}}{2E_{\psi}} \end{aligned} \quad (17)$$

with

$$|C_f| = \frac{G_F}{\sqrt{2}} |V_{cb}| |V_{cf}| M_{\psi} f_{\psi} |a_2|. \quad (18)$$

Here the modification from the field-theoretical approach simply enters in form of the step-function $\varepsilon(x)$ which exactly provides the additional terms $f(x_-)$ in the tensor coefficients (14). Evaluating Eq. (17) in the restframe of the B meson we arrive at the formula for the J/ψ momentum spectrum,

$$\frac{d\Gamma_{(B \rightarrow J/\psi X)}}{d|\vec{k}_\psi|} = \sum_{f=s,d} \frac{|C_f|^2}{4\pi M_B} \left[3W_1 + W_2 \frac{|\vec{k}_\psi|^2}{M_\psi^2} \right] \frac{|\vec{k}_\psi|^2}{E_\psi}, \quad (19)$$

within the framework of the inclusive parton model. Using Eq. (14) the corresponding differential branching ratio can be written as

$$\begin{aligned} \frac{1}{\Gamma_B} \frac{d\Gamma_{(B \rightarrow J/\psi X)}}{d|\vec{k}_\psi|} (|\vec{k}_\psi|, |\vec{p}_B| = 0) = \\ \tau_B \sum_{f=s,d} \frac{|C_f|^2}{2\pi M_B} \frac{|\vec{k}_\psi|^2}{E_\psi} \left[f(x_+) \left(1 + \frac{2E_\psi M_B}{M_\psi^2} \left(x_+ - \frac{2m_f^2}{M_B^2(x_+ - x_-)} \right) \right) + (x_+ \leftrightarrow x_-) \right], \end{aligned} \quad (20)$$

within the kinematical range

$$M_\psi \leq E_\psi \leq \frac{M_B^2 + M_\psi^2 - S_{min}^{(f)}}{2M_B}, \quad S_{min}^{(f)} = m_f^2. \quad (21)$$

To compare our result (20) with data from CLEO a Lorentz boost has in addition to be performed from the restframe of the B meson to a B produced at the $\Upsilon(4S)$ resonance ($|\vec{p}_B| = 0.34$ GeV). The explicit form of the boost integral we give in Section 3.1 in the context of the ACCMM model (see Eq. (33)).

All terms are known in this decay except for the product $(|a_2|f_\psi)$ and the structure function which occurs with two arguments. We note that when neglecting the small $f(x_-)$ contribution the decay spectrum is directly proportional to $f(x_+)$. Thus measuring the momentum spectrum of the J/ψ we can read from the data the distribution function. The extraction of $f(x_+)$ is direct, in contrast to the extraction from the electron energy spectrum in the semileptonic decay of the B meson which involves an integral over the structure function.

In the following Section we compare the predictions of Eq. (20) with the existing experimental data.

2.2 Analysis and Numerical Evaluation

The probability distribution function (16) is not Lorentz invariant and is defined in the infinite momentum frame. It cannot be transformed to the restframe of the B meson (or

a frame which corresponds to a B meson produced at the $\Upsilon(4s)$ resonance), because it involves an infinite sum of quark-antiquark pairs whose calculation requires a complete solution of the field-theory. In the absence of direct measurements of the distribution function we use a one-parameter Ansatz and fix the distribution parameter by comparing our results with data. Referring to theoretical studies which pointed out that the distribution and fragmentation function of heavy quarks peak at large values of x [33, 34], as a working hypothesis we assume that the functional form of both is similar. The latter is known from experiment and we shall use the Peterson functional form [35–37]

$$f_\varepsilon(x) = N_\varepsilon \frac{x(1-x)^2}{[(1-x)^2 + \varepsilon_p x]^2}, \quad (22)$$

with ε_p being the free parameter and N_ε the corresponding normalization constant. This form we already applied in the semileptonic decays of the B meson [11, 12].

In Fig. 2a we show the distribution function $f_\varepsilon(x)$ for various values of ε_p . The kinematical range for the two arguments $x_\pm(m_f)$ of the distribution function according to Eq. (21) reads

$$\frac{M_\psi + m_f}{M_B} \leq x_+ \leq 1, \quad \frac{M_\psi^2 - m_f^2}{M_B^2} \leq x_- \leq \frac{M_\psi - m_f}{M_B}. \quad (23)$$

As pointed out in Fig. 3 the variable x_- only occurs with values at which $f_\varepsilon(x_-)$ is small. Therefore the corresponding contribution to the differential branching ratio (20) is small.

We use the distribution (22) to fit the measured momentum spectrum of the J/ψ which was given by the CLEO group [9]. As argued above we fix $f_\psi = 0.384$ GeV and vary $|a_2|$ according to the range covered by the various models for exclusive decays.

The shape of the theoretical spectrum is determined by the distribution parameter ε_p , which is illustrated in Fig. 4 where we show the spectrum for $|a_2| = 0.275$ and several values of ε_p . A general feature of the analysis is our difficulty in reproducing the data over the whole range of phase-space. Confronted with this problem, we lay greater emphasis on the appropriate description of the *low* momentum range ($|\vec{k}_\psi| \leq 1.4$ GeV) in our simultaneous fits of $|a_2|$, which in this decay has the meaning of a pure normalization constant, and the distribution parameter ε_p . Within this region the J/ψ spectrum obtains a sizable contribution from decay channels containing three or more particles in the final state (where higher K^* resonances are assumed to be unimportant), whereas the high momentum range is purely determined by the exclusive two-body decays $B \rightarrow J/\psi K^{(*)}$. Therefore incoherence as a necessary ingredient of the IPM is limited to the former region.

Furthermore we demand the reproduction of the measured branching ratio for the decay under consideration. Thus if we apply small values for the distribution parameter

$\varepsilon_p \leq 0.006$ we cannot account for the low momentum region, which is underestimated significantly within the theoretical spectrum (see Fig. 5). On the other hand, demanding the reproduction of the branching ratio, a distribution corresponding to $\varepsilon_p \geq 0.010$ would imply a value $|a_2| \geq 0.30$, which is beyond the range given from the study of exclusive two-body decays. Therefore, in spite of the difficulty to reproduce the data accurately over the whole range of phase-space, the investigation of the decay $B \rightarrow J/\psi X$ is more restrictive with regard to the distribution parameter than the semileptonic decay of the B meson which involves an integral over the structure function.

Considering the fact that the IPM does not include hadronization effects and consequently yields an averaged spectrum, a satisfactory description of the dataset is achieved for $\varepsilon_p = \mathcal{O}(0.008)$, $|a_2| = \mathcal{O}(0.285)$ (compare Fig. 5) when using current masses for the final state quarks. Applying constituent masses would involve an incorrect position of the maximum of the momentum spectrum and, in addition, a sizable underestimate of the high momentum range (see Fig. 6). Yet also for $\varepsilon_p = 0.008$ there is apparent a moderate systematic underestimate of the latter region. Since the model presumes the existence of multiple final states it may not hold for the high momentum range ($|\vec{k}_\psi| \geq 1.4$ GeV) where two-body decays determine the spectrum. Following the CLEO analysis, as a trial we subtract the expected contribution of the exclusive decays $B \rightarrow K^{(*)} J/\psi$ from the data for the semi-inclusive momentum spectrum. Carrying out the fit for this modified momentum distribution we observe that the agreement between theory and experiment is improved for large values of the distribution parameter $\varepsilon_p \geq 0.012$ (however only when applying constituent masses for the final state quarks), corresponding to a soft momentum distribution of the heavy quark. In Fig. 7 we show the modified spectrum for $|a_2| = 0.275$ and ε_p as stated there. This additional fit may serve as an indication that a value $\varepsilon_p = \mathcal{O}(0.014)$ has to be suggested within the model when restricting the analysis of decay spectra to the ‘incoherence region’ where multi-particle final states exist. Then additional information from a model describing the dominant two-body decay channels has to be implemented to reproduce the data over the whole range of phase-space.

Finally, the errors in the data, although substantially improved, are still significant and a crucial test will be possible, when the error bars are further reduced. It is of special interest to establish whether the deviations at $|\vec{k}_\psi| \simeq 0.5$ GeV from the smooth shape of the spectrum, which is predicted in our inclusive approach, survive and to extend the analysis of the composition, in terms of resonances and continuum, for $|\vec{k}_\psi| \geq 1.4$ GeV.

3 $B \rightarrow J/\psi X$ in the ACCMM Model

3.1 Calculation of the Differential Branching Ratio

A second approach which allows us to determine the momentum distribution of the J/ψ in the semi-inclusive decay of the B meson is given through the ACCMM model [16]. In this model the bound state corrections to the simple quark picture are incorporated by attributing to the spectator quark a Fermi motion within the meson. The momentum spectrum of the J/ψ is then obtained by folding the Fermi motion with the spectrum from the b quark decay. In Ref. [38] the shape of the J/ψ momentum distribution resulting from Fermi momentum smearing has been given in the restframe of the B meson, but without a comparison with data, and without consideration of the light spectator quark mass. Moreover the authors applied the constituent mass for the strange quark in the final state, whereas we will show that a satisfactory reproduction of the data can only be obtained applying the current mass.

According to Eq. (5) the J/ψ is treated as a color singlet current using the factorization assumption of Eq. (4). The spectator quark is handled as on-shell particle with definite mass m_{sp} and momentum $|\vec{p}| = p$. Consequently, the b quark is considered to be off-shell with a virtual mass W given in the restframe of the B meson by energy-momentum conservation as

$$W^2(p) = M_B^2 + m_{sp}^2 - 2M_B\sqrt{m_{sp}^2 + p^2}. \quad (24)$$

Altarelli et al. introduced in the model a gaussian probability distribution $\phi(p)$ for the spectator (and thus for the heavy quark) momentum,

$$\phi(p) = \frac{4}{\sqrt{\pi}p_f^3} \exp\left(-p^2/p_f^2\right), \quad (25)$$

normalized according to

$$\int_0^\infty dp p^2 \phi(p) = 1. \quad (26)$$

Here a free parameter p_f is adopted for the gaussian width which has to be determined by experiment.

The main difference between the inclusive parton model and ACCMM is that the latter one must consider a b quark in flight. We therefore start from the momentum spectrum of the J/ψ resulting from the decay $b \rightarrow q_f J/\psi$ ($f = s, d$) of a b quark of mass W and momentum p which is given by

$$\frac{d\Gamma_b^{(f)}}{d|\vec{k}_\psi|}(|\vec{k}_\psi|, p) = \gamma_b^{-1} \frac{\Gamma_0^{(f)}}{k_+^{(b,f)}(p) - |k_-^{(b,f)}(p)|} \left[\theta\left(|\vec{k}_\psi| - |k_-^{(b,f)}(p)|\right) - \theta\left(|\vec{k}_\psi| - k_+^{(b,f)}(p)\right) \right]. \quad (27)$$

Here we have defined

$$\theta(x) = \begin{cases} 1, & x > 0 \\ 0, & x < 0. \end{cases} \quad (28)$$

$\Gamma_0^{(f)}$ is the width of the analogous decay in the restframe of the heavy quark where we have confined ourselves to the leading order result,

$$\Gamma_0^{(f)} = \frac{|C_f|^2 k_0^{(f)}}{2\pi W^2} \left[m_f^2 + \frac{1}{2} (W^2 - m_f^2 - M_\psi^2) \left(2 + \frac{W^2 - m_f^2}{M_\psi^2} \right) \right], \quad (29)$$

with $|C_f|$ according to Eq. (18) and with the momentum $k_0^{(f)}$ of the J/ψ ,

$$k_0^{(f)} = \frac{1}{2W} \left[(W^2 - m_f^2 + M_\psi^2)^2 - 4W^2 M_\psi^2 \right]^{\frac{1}{2}}, \quad E_0^{(f)} = \sqrt{k_0^{(f)2} + M_\psi^2}. \quad (30)$$

For a vanishing mass m_f of the final quark Eq. (29) is equivalent to Eq. (5) in Ref. [3].

In Eq. (27) $k_\pm^{(b,f)}$ give the limits of the momentum range which results from the Lorentz boost from the restframe of the b quark to a frame where the b has a nonvanishing momentum p ,

$$k_\pm^{(b,f)}(p) = \frac{1}{W} (E_b k_0^{(f)} \pm p E_0^{(f)}), \quad (31)$$

and γ_b^{-1} is the corresponding Lorentz factor,

$$\gamma_b^{-1} = \frac{W}{E_b}, \quad E_b = \sqrt{W^2 + p^2}. \quad (32)$$

To calculate the momentum spectrum of the J/ψ from the semi-inclusive decay of the B meson one has to fold the heavy quark momentum probability distribution with the spectrum (27) resulting from the quark subprocess. Performing this we finally arrive at the expression for the differential branching ratio for a B meson in flight,

$$\begin{aligned} \frac{1}{\Gamma_B} \frac{d\Gamma_{(B \rightarrow J/\psi X)}}{d|\vec{k}_\psi|} (|\vec{k}_\psi|, |\vec{p}_B|) = \\ \tau_B \sum_{f=s,d} \int_{|k_-^{(f)}|}^{k_+^{(f)}(|\vec{k}_\psi|)} \frac{d|\vec{k}'_\psi|}{k_+^{(f)}(|\vec{k}'_\psi|) - |k_-^{(f)}(|\vec{k}'_\psi|)|} \int_0^{p_{max}^{(f)}} dp p^2 \phi(p) \frac{d\Gamma_b^{(f)}}{d|\vec{k}_\psi|} (|\vec{k}'_\psi|, p). \end{aligned} \quad (33)$$

Here $p_{max}^{(f)}$ is the maximum kinematically allowed value of the quark momentum p , i.e., that which makes W in Eq. (24) equal to $W = m_f + M_\psi$,

$$p_{max}^{(f)} = \frac{1}{2M_B} \left[(M_B^2 + m_{sp}^2 - (m_f + M_\psi)^2)^2 - 4m_{sp}^2 M_B^2 \right]^{\frac{1}{2}}. \quad (34)$$

The first integration in Eq. (33) results from the transformation from the spectrum for a B meson at rest to the spectrum for a B meson in flight, where

$$k_{\pm}(|\vec{k}_{\psi}|) = \frac{1}{M_B} \left(E_B |\vec{k}_{\psi}| \pm |\vec{p}_B| E_{\psi} \right), \quad k_+^{(f)}(|\vec{k}_{\psi}|) = \min\{k_+(|\vec{k}_{\psi}|), k_{max}^{(f)}\}, \quad (35)$$

$k_{max}^{(f)}$ being the maximum value of the J/ψ momentum from the decay $B \rightarrow J/\psi X_f$ in the restframe of the B ,

$$k_{max}^{(f)} = \frac{1}{2M_B} \left[\left(M_B^2 + M_{\psi}^2 - S_{min}^{(f)} \right)^2 - 4M_B^2 M_{\psi}^2 \right]^{\frac{1}{2}}, \quad S_{min}^{(f)} = (m_f + m_{sp})^2. \quad (36)$$

In the following Section we make use of Eq. (33) to compare the model predictions with experimental data.

3.2 Analysis and Numerical Evaluation

Both models, the inclusive parton model as well as the ACCMM model incorporate the bound state structure of the B meson by postulating a momentum distribution for the heavy quark. Introducing in the latter model another x -variable as the ratio $x = W/M_B$, the appropriate distribution function for the relative mass fraction $w(x)$ of the b quark in the restframe of the B meson is given as

$$\begin{aligned} w(x) &= \frac{2M_B^2}{\sqrt{\pi} p_f^3} p(x) x \left(1 - x^2 + \frac{m_{sp}^2}{M_B^2} \right) \exp \left[-p(x)^2 / p_f^2 \right], \\ p(x) &= \frac{M_B}{2} \left[(1 - x^2)^2 - 2 \frac{m_{sp}^2}{M_B^2} (1 + x^2) + \frac{m_{sp}^4}{M_B^4} \right]^{\frac{1}{2}}, \end{aligned} \quad (37)$$

where the corresponding normalization reads

$$\int_0^{1-m_{sp}/M_B} w(x) dx = 1. \quad (38)$$

In Fig. 2b we show the distribution function $w(x)$ for $m_{sp} = 0.2$ GeV and various values of p_f . From Eqs. (37) one realizes that for given on-shell masses the Fermi parameter p_f determines the average value $\langle W \rangle = M_B \langle x \rangle$ of the virtual b quark mass and hence also the total decay width.

Both models have the advantage of avoiding the mass of the heavy quark as an independent parameter. As a consequence, the phase-space is treated correctly by means of using mesonic degrees of freedom. Nevertheless the endpoint of the phase-space in the ACCMM model is slightly different from that in the IPM because of the on-shell mass

m_{sp} of the spectator quark from which the minimal invariant mass square of the hadronic system $S_{min}^{(f)}$ results as given in Eq. (36).

The shape of the momentum spectrum in the decay $B \rightarrow J/\psi X$ is mainly determined by the value of p_f . The extraction of this value from a comparison with experimental data is important not only for explaining the decay itself and thus testing the factorization assumption of Eq. (4), but also for the determination of $|V_{ub}/V_{cb}|$ from the endpoint region of the inclusive *semileptonic* $B \rightarrow X_{c(u)} l \nu$ decay spectrum. As recently stressed in Ref. [39] the experimental extraction of p_f from semileptonic decays has been ambiguous, because various parameters of the model were fitted simultaneously to the lepton energy spectrum where in addition the perturbative QCD corrections are important in the endpoint region (especially for $b \rightarrow u$). Furthermore, as stated in Ref. [25], for a large range of the phase-space the bound state corrections are of minor importance in this decay channel.

Whereas usually $p_f = 0.3$ GeV is used for the data analysis the authors of Ref. [39] calculate the Fermi parameter theoretically in the relativistic quark model and obtain $p_f = 0.54$ GeV. A CLEO analysis [40] of the endpoint lepton spectrum in the semileptonic decay channel employing the common value $p_f = 0.3$ GeV (and $m_{sp} = 0.15$ GeV) yields a discrepancy between the ACCMM and the ISGW model of *Isgur et al.* [41] in the determination of $|V_{ub}/V_{cb}|$,

$$\begin{aligned} 10^2 \times |V_{ub}/V_{cb}|^2 &= 0.57 \pm 0.11 && (\text{ACCMM}) \\ &= 1.02 \pm 0.20 && (Isgur et al.). \end{aligned} \quad (39)$$

Using however $p_f = 0.5$ GeV the authors of Ref. [39] arrive at the value $10^2 \times |V_{ub}/V_{cb}|^2 = 1.03$ within the ACCMM model, obtaining a good agreement with the ISGW model.

The decay $B \rightarrow J/\psi X$ provides an independent way of extracting the Fermi parameter p_f . In contrast to the lepton spectrum in the semileptonic decay the shape of the J/ψ momentum spectrum is highly sensitive to this parameter over the whole phase-space. This is analogous to the determination of the parameter ε_p in Section 2.2.

Employing the spectator distribution function (25) we calculated the momentum spectrum for the decay of B mesons produced at the $\Upsilon(4s)$ resonance. Fig. 8 shows the comparison with the CLEO data for $f_\psi = 0.384$ GeV, $m_{sp} = 0.2$ GeV, $m_s = 0.125$ GeV, $m_d = 0$ and various sets of values for p_f and $|a_2|$ as stated there. Here we want to emphasize that analogous to the IPM the best fit is achieved when employing current masses for the final state quarks. This is a consequence of the fact that within the theory these are treated as free particles without consideration of fragmentation. The application of constituent masses would yield a sizable underestimate of the high momentum region (see Fig. 9).

In addition to the final state quark masses m_f the spectator mass also determines the range of phase-space and the position of the maximum (compare Fig. 10). The latter is in accordance with the data for $m_{sp} = 0.2$ GeV.

In Fig. 8 one can see that the agreement of the theoretical spectrum with the data is very good provided we choose the value $p_f = \mathcal{O}(0.55 \text{ GeV})$. To demonstrate the high sensitivity of the spectrum on this parameter over the whole range of phase-space we present in Fig. 11 spectra for different values of p_f with f_ψ and $|a_2|$ fixed. It is obvious that the shape of the experimental J/ψ momentum distribution (compare Fig. 8) cannot be reproduced in the model when using values for the Fermi motion parameter significantly smaller than $p_f = 0.5$ GeV. Especially the sizable contribution in the low momentum range requires a soft probability distribution of the heavy quark momentum.

As a result, we conclude that the value $p_f = \mathcal{O}(0.55 \text{ GeV})$ for the Fermi motion parameter of the ACCMM model is highly favoured when applying this model to the semi-inclusive decay $B \rightarrow J/\psi X$. This value is in exact accordance with the one calculated recently in Ref. [39] from the relativistic quark model. As mentioned above the discrepancy between the ACCMM model and the ISGW model concerning the determination of $|V_{ub}/V_{cb}|$ disappears when using our favoured value for p_f in the study of the electron spectrum from inclusive semileptonic B decays.

A final feature of our investigations is related to the determination of the effective color singlet coefficient $|a_2|$. Using $f_\psi = 0.384 \text{ GeV}$, $\tau_B = 1.54 \text{ ps}$, and $|V_{cb}| = 0.043$, we obtain $|a_2| = \mathcal{O}(0.28)$ for the best fit of the ACCMM model to the CLEO data. This is in agreement to the value of $|a_2|$ which we found in the IPM. The study of an inclusive decay compared to exclusive decays in this context provides the advantage of solely involving an analysis that is independent of mesonic form-factors.

4 Remarks on the Extraction of $|V_{ub}/V_{cb}|$

The application of the value for p_f , which we obtain from our investigation of the decay $B \rightarrow J/\psi X$, to the semileptonic decay channel requires some additional remarks. As pointed out in Ref. [42] the universality of the momentum distribution function describing the motion of the b quark in the B meson only holds for different decay processes when referring to a fixed final state quark mass.

The common procedure, followed in the analysis of the semileptonic decay $B \rightarrow X l \nu$, is to determine the distribution parameter from a fit of the lepton spectrum away from the endpoint where the spectrum is dominated by $b \rightarrow c$ transitions. This result is then used

to model the endpoint region, which purely originates from $b \rightarrow u$ transitions, in order to extract the value of $|V_{ub}/V_{cb}|$ from the data. Considering however the fact that the decay $b \rightarrow c$ involves a quark mass m_c , which cannot be neglected, the corresponding distribution parameter might be unsuitable to describe simultaneously the transition $b \rightarrow u$.

On the other hand, the independent determination of the heavy quark momentum distribution from the entire J/ψ spectrum of the $B \rightarrow J/\psi X$ decay involves the effective transition $b \rightarrow s$ (and also the Cabibbo suppressed decay $b \rightarrow d$), i.e., a small (current) mass for the final state. Therefore the corresponding distribution parameter is still appropriate for the extraction of $|V_{ub}/V_{cb}|$, which requires the distribution function associated with the transition to a massless final state.

The CLEO analysis [40] was performed within the ACCMM model using the value $p_f = 0.3$ GeV for both, $b \rightarrow c$ and $b \rightarrow u$ decays. The modification which arises when keeping this value for the transition $b \rightarrow c$ but applying $p_f = 0.5$ GeV for $b \rightarrow u$ reads

$$\left| \frac{V_{ub}}{V_{cb}} \right|_{p_f=0.5}^2 = \left| \frac{V_{ub}}{V_{cb}} \right|_{p_f=0.3}^2 \times \frac{\tilde{\Gamma}(p_f = 0.3)}{\tilde{\Gamma}(p_f = 0.5)}, \quad (40)$$

where $\tilde{\Gamma}(p_f) \equiv \int_{2.3}^{2.6} dE_l \frac{d\Gamma}{dE_l}(p_f)$ denotes the integration over the endpoint domain of the leptonic spectrum supposing $|V_{ub}| = 1$. This is exactly the same relation which has been used in Ref. [39] and we quote the corresponding value for $|V_{ub}/V_{cb}|^2$ in Section 3.2. Nevertheless the physical interpretation is somewhat different. The authors of Ref. [39] took the value of $|V_{cb}|$ as determined independently from other analyses. This appeared to be necessary, because they did not consider the limitations to the universality of the distribution function arising from different masses of the final state quark. In contrast to this we argue that Eq. (40) can be applied directly in the investigation of the semileptonic spectrum, since only the distribution parameter governing the endpoint region has to be changed relative to the existing CLEO analysis [40]. Within this analysis the application of the ACCMM model to $b \rightarrow c$ transitions has to be regarded as a phenomenological fit, because from a theoretical point of view the neglect of Fermi motion in the final state is only appropriate, when small final state quark masses are involved [42].

The latter remark illustrates the importance of a study which is independent of the semileptonic data. Our investigation of the decay $B \rightarrow J/\psi X$ allows a suitable determination of the parameters of the ACCMM model which can be used for the analysis of the endpoint spectrum in the decay $B \rightarrow X l \nu$. The same statement holds true for our analysis within the parton model.

5 Polarization of the J/Ψ

Applying the same method as for the calculation of the unpolarized J/ψ spectrum, we proceed to determine the momentum spectrum of a longitudinally polarized state.

In references [5] and [10] the polarization of the J/ψ was obtained from a study of the free quark decay $b \rightarrow J/\psi s$, i.e., for fixed momenta in the final state. The result, $\Gamma_L/\Gamma \simeq 0.54$, was identified with the average polarization in the corresponding decay of the B meson. Considering the bound state structure of the B within our inclusive approach yields the momentum distribution of the J/ψ . Consequently, it allows us to determine the polarization in various kinematic regions, where the results can be compared with measurements from CLEO [43] and ARGUS [44].

Since our model is based on local quark-hadron duality, we do not expect to reproduce the polarization within the region $|\vec{k}_\psi| \geq 1.4$ GeV, because it is governed by the two-body decay modes $B \rightarrow J/\psi K^{(*)}$. As can be concluded from the ARGUS data (see Tab. 1), after subtraction of the exclusive mode $B \rightarrow J/\psi K$ the high momentum range of the decay spectrum is dominated by a single orbital angular momentum and consequently by a single CP eigenstate of the mode $B \rightarrow J/\psi K^*$ [45]. This feature is not accounted for within our inclusive approach since final state interactions are not part of our consideration.

Nevertheless the study of the low momentum range, which involves nonresonant multi-particle states, provides an additional test of our approach, especially in view of future measurements with reduced experimental errors. Furthermore we investigate the modification of the average polarization relative to the free quark decay due to the bound state structure of the B , in which the hadronic vertex acts on the polarization of the J/ψ through the momentum distribution of the underlying b quark.

Replacing the polarization sum in Eq. (9) by $\varepsilon_\mu(\lambda=0)\varepsilon_\nu(\lambda=0)$, a calculation analogous to the determination of the unpolarized $B \rightarrow J/\psi X$ decay spectrum within the parton model, introduced in Section 2, yields the momentum spectrum for the longitudinally polarized J/ψ . In the restframe of the B ,

$$\frac{1}{\Gamma_B} \frac{d\Gamma_{(B \rightarrow (J/\psi)_L X)}}{d|\vec{k}_\psi|} (|\vec{k}_\psi|, |\vec{p}_B| = 0) = \quad (41)$$

$$\tau_B \sum_{f=s,d} \frac{|C_f|^2}{2\pi M_B} \frac{|\vec{k}_\psi|^2}{E_\psi} \left[f(x_+) \left(-1 + \frac{2E_\psi M_B}{M_\psi^2} \left(x_+ - \frac{2m_f^2}{M_B^2(x_+ - x_-)} \right) \right) + (x_+ \leftrightarrow x_-) \right],$$

with $|C_f|$ defined according to Eq. (18). Note that the difference to the unpolarized spectrum occurs in the first term in the parenthesis of Eq. (41), whose sign changes compared

to Eq. (20). The partial branching ratio in the CLEO frame is obtained by performing the integration due to the transformation of the spectrum to that for a B meson in flight (see Eq. (33)), as well as the integration over the momentum range which is considered.

The calculation in the ACCMM model follows the lines of Section 3, where for the polarized case Eq. (29) is replaced by the corresponding expression for the decay width of $b \rightarrow (J/\psi)_L q_f$. In the restframe of the heavy quark one obtains

$$\Gamma_{0,L}^{(f)} = \frac{|C_f|^2 k_0^{(f)}}{2\pi W^2} \left[-m_f^2 + \frac{1}{2} (W^2 - m_f^2 - M_\psi^2) \left(\frac{W^2 - m_f^2}{M_\psi^2} \right) \right]. \quad (42)$$

The partial branching ratio for the momentum range $k_1 \leq |\vec{k}_\psi| \leq k_2$ then reads

$$\Delta B_{[L]}(k_1, k_2) = \tau_B \sum_{f=s,d} \int_{k_1}^{k_2} d|\vec{k}_\psi| \int_0^{p_{max}^{(f)}} dp \frac{p^2 \phi(p) \gamma_b^{-1} \Gamma_{0[L]}^{(f)}}{k_+^{(b,f)}(p) - |k_-^{(b,f)}(p)|} \int_{g_1(|\vec{k}_\psi|, p)}^{g_2(|\vec{k}_\psi|, p)} \frac{d|\vec{k}'_\psi|}{k_+(|\vec{k}'_\psi|) - |k_-(|\vec{k}'_\psi|)|}, \quad (43)$$

where

$$g_1(|\vec{k}_\psi|, p) = \max \left\{ |k_-(|\vec{k}_\psi|)|, |k_-^{(b,f)}(p)| \right\} h(|\vec{k}_\psi|, p), \quad (44)$$

$$g_2(|\vec{k}_\psi|, p) = \min \left\{ k_+(|\vec{k}_\psi|), k_+^{(b,f)}(p) \right\} h(|\vec{k}_\psi|, p), \quad (45)$$

and

$$h(|\vec{k}_\psi|, p) = \theta \left[k_+^{(f)}(|\vec{k}_\psi|) - |k_-^{(b,f)}(p)| \right] \theta \left[k_+^{(b,f)}(p) - |k_-(|\vec{k}_\psi|)| \right]. \quad (46)$$

In Eqs. (43-46) the limits of integration are written in a way as to take into account simultaneously the Lorentz boost from the b to the B restframe and the subsequent boost to the CLEO frame.

Our results for the average longitudinal polarization of the J/ψ , $\Gamma_L/\Gamma = \Delta B_L/\Delta B$, are presented in Tab. 1. There we give the polarization obtained in the parton and the ACCMM model for different values of the quark momentum distribution parameters ε_p and p_f , respectively. The J/ψ momentum ranges that we considered are chosen according to the experimental data from ARGUS and CLEO. From the table one can read that in both models the data is reproduced correctly for the range $|\vec{k}_\psi| \leq 1.4$ GeV and also for the average over the complete momentum range. The agreement is good, but the experimental errors are still large. On the other hand, the polarization predicted for the high momentum region underestimates the data. This is to be expected because, as we mentioned, the region $|\vec{k}_\psi| > 1.4$ GeV is dominated by two-body modes.

J/ψ momentum	CLEO II [43]	ARGUS [44]
$k_\psi < 0.8$ GeV	0.55 ± 0.35	
$0.8 \text{ GeV} < k_\psi < 1.4$ GeV	0.49 ± 0.32	
$1.4 \text{ GeV} < k_\psi < 2.0$ GeV	0.78 ± 0.17	1.17 ± 0.17
all $k_\psi < 2.0$ GeV	0.59 ± 0.15	

parton model				
J/ψ momentum	$\varepsilon_p = 0.004$	$\varepsilon_p = 0.006$	$\varepsilon_p = 0.008$	$\varepsilon_p = 0.010$
$k_\psi < 0.8$ GeV	0.416	0.415	0.414	0.413
$0.8 \text{ GeV} < k_\psi < 1.4$ GeV	0.520	0.515	0.512	0.508
$1.4 \text{ GeV} < k_\psi < 2.0$ GeV	0.557	0.552	0.547	0.543
all $k_\psi < 2.0$ GeV	0.537	0.529	0.522	0.516

ACCMM model				
J/ψ momentum	$p_f = 0.3$	$p_f = 0.4$	$p_f = 0.5$	$p_f = 0.55$
$k_\psi < 0.8$ GeV	0.515	0.504	0.495	0.491
$0.8 \text{ GeV} < k_\psi < 1.4$ GeV	0.548	0.538	0.530	0.527
$1.4 \text{ GeV} < k_\psi < 2.0$ GeV	0.556	0.549	0.542	0.539
all $k_\psi < 2.0$ GeV	0.553	0.543	0.534	0.529

Table 1: J/ψ polarization Γ_L/Γ in the decay $B \rightarrow J/\psi X$ in the parton and the ACCMM model compared to data. The parameters are $m_{sp} = 0.2$ GeV, $m_s = 0.125$ GeV, $m_d = 0$, and ε_p, p_f [GeV] respectively, as given above.

Significant differences between the parton and the ACCMM model show up only for the low momentum range ($|\vec{k}_\psi| \leq 0.8$ GeV), which may provide an additional feature for distinguishing between the models. The bound state corrections to the average polarization of the J/ψ (for all $|\vec{k}_\psi| \leq 2.0$ GeV) are marginal; a property which is reflected in the weak dependence of the polarization on the distribution parameters. As a consequence of the cancellation of binding effects in the ratio $\Delta B_L/\Delta B$, the determination of ε_p and p_f , respectively, from the polarization turns out to be impossible.

We conclude that the inclusive approach to $B \rightarrow J/\psi X$ decays in the parton and the ACCMM model yields the polarization of the J/ψ in various kinematic regions. Our analysis shows that for the high momentum range, in which final state interactions are

important, the approach is less reliable in the polarized than in the unpolarized case. On the other hand, the inclusive description is well suited in the low momentum range governed by nonresonant multi-particle states. A study of the polarization in this range may help distinguishing between the models considered, as soon as the experimental error is reduced.

6 Summary and Conclusion

We incorporate in this article the bound state effects of the B meson in the analysis of the direct decay $B \rightarrow J/\psi X$. An inclusive approach has been worked out in detail within the framework of the parton and the ACCMM model where in each case a one-parameter momentum distribution function for the heavy quark is introduced. We fixed the distribution parameter by comparing the predicted J/ψ momentum spectrum with the recent CLEO data, putting emphasis on the adequate reproduction of the sizable low momentum spectrum, which contains nonresonant multi-particle final states. Both models yield a b quark momentum distribution softer than the one commonly used in studies of semileptonic B decays. Within the parton model we obtain $\varepsilon_p = \mathcal{O}(0.008)$ where moderate deviations from the Peterson *et al.* distribution, taken from production experiments, are apparent in the data. In further studies of inclusive B decays within the parton model it will be of interest to consider a modified Ansatz for the b quark momentum distribution.

The ACCMM model can account for the data over the whole range of phase-space when we use a Fermi motion parameter $p_f = \mathcal{O}(0.5 \text{ GeV})$. Applying this result to the endpoint electron energy spectrum of semileptonic B meson decays yields a value $10^2 \times |V_{ub}/V_{cb}|^2 = 1.03$, which is in accordance to the result obtained within the exclusive ISGW model.

The successful reproduction of the experimental data confirms the validity of the factorization assumption for inclusive B decays where the bound state effects in both models imply a large value for the effective color singlet coefficient, $|a_2| = \mathcal{O}(0.28)$ (when choosing $\tau_B = 1.54 \text{ ps}$, $|V_{cb}| = 0.043$). The inclusive approach can also account for the measured average polarization of the J/ψ which is independent of the normalization constants ($|a_2|f_\psi$) and τ_B .

In view of the fact that semileptonic decay spectra away from the endpoint of the phase-space involve $b \rightarrow c$ transitions a study of the decay $B \rightarrow J/\psi X$ presently provides the only possibility to extract the momentum distribution of the b quark corresponding to a decay in which the mass of the quark in the final state is negligible. This extraction is direct as no integration over the distribution function has to be performed. Furthermore

the momentum spectrum of the J/ψ is more sensitive to the bound state structure of the B than the electron energy spectrum from semileptonic decays. The difficulties which arise in the study of a momentum spectrum containing resonance structures can be avoided as soon as precise measurements are available which allow a determination of the distribution function from the endpoint domain of the electron energy spectrum in semileptonic decays or the photon spectrum in $b \rightarrow s \gamma$ decays.

Acknowledgements

PHS wants to thank the *Deutsche Forschungsgemeinschaft* for financial support (in connection with the Graduate College for Elementary Particle Physics in Dortmund).

References

- [1] G. Bodwin, E. Braaten, T.C. Yuan, and G.P. Lepage, Phys. Rev. **D 46**, (1992) 3703.
- [2] P. Ko, J. Lee, and H.S. Song, preprint SNUTP 95-064 (1995).
- [3] M.B. Wise, Phys. Lett. **B 89**, (1980) 229.
- [4] J.H. Kühn, S. Nussikov, and R. Rückl, Z. Phys. **C 5**, (1980) 117.
- [5] J.H. Kühn and R. Rückl, Phys. Lett. **B 135** (1984) 477; Erratum-ibid. **258**, (1991) 499.
- [6] L. Bergström and P. Ernström, Phys. Lett. **B 328**, (1994) 153.
- [7] H. Albrecht *et al.* (ARGUS Collaboration), Phys. Lett. **B 199**, (1987) 451.
- [8] D. Bortoletto *et al.* (CLEO Collaboration), Phys. Rev. **D 45**, (1992) 21.
- [9] R. Fulton *et al.* (CLEO Collaboration), Phys. Rev. **D 52**, (1995) 2661.
- [10] W.F. Palmer and B. Stech, Phys. Rev. **D 48**, (1993) 4174.
- [11] C.H. Jin, W.F. Palmer, and E.A. Paschos, Phys. Lett. **B 329**, (1994) 364.
- [12] C.H. Jin, W.F. Palmer, and E.A. Paschos, preprint DO-TH 93/21 and OHSTPY-HEP-T-93-011, (1993) (unpublished).
- [13] C.H. Jin and E.A. Paschos, preprint DO-TH 95/07.
- [14] A. Bareiss and E.A. Paschos, Nucl. Phys. **B 327**, (1992) 311.
- [15] A. Bareiss, Z. Phys. **C 53**, (1989) 353.
- [16] G. Altarelli, N. Cabibbo, G. Corbò, L. Maiani, and G. Martinelli, Nucl. Phys. **B 208**, (1982) 365.
- [17] For reviews see:
T. Mannel, in *QCD- 20 Years Later*, edited by P.M. Zerwas and H.A. Kastrup (World Scientific, Singapore, 1993);
M. Neubert, Phys. Rept. **245**, (1994) 259.
- [18] J. Chay, H. Georgi, and B. Grinstein, Phys. Lett. **B 247**, (1990) 399.

- [19] I. Bigi and N.G. Uraltsev, Phys. Lett. **B 280**, (1992) 120.
- [20] I. Bigi, N.G. Uraltsev, and A. Vainshtein, Phys. Lett. **B 293**, (1992) 430; Erratum-
ibid. **297**, (1993) 477.
- [21] M. Neubert, Phys. Rev. **D 49**, (1994) 1542.
- [22] T. Mannel, Proceedings of the 138th WE-Heraeus Seminar, edited by J.G. Körner
and P. Kroll (World Scientific, 1995).
- [23] I. Bigi, M. Shifman, N.G. Uraltsev, and A. Vainshtein, Phys. Rev. **D52**, (1995) 196.
- [24] I. Bigi, M. Shifman, N.G. Uraltsev, and A. Vainshtein, Phys. Rev. Lett. **71**, (1993)
496.
- [25] C. Csáki and Lisa Randall, Phys. Lett. **B 324**, (1994) 451.
- [26] A. Buras and P.H. Weisz, Nucl. Phys. **B 333**, (1990) 66.
- [27] M. Wirbel, B. Stech, and M. Bauer, Z. Phys. **C 29**, (1985) 637.
- [28] M.S. Alam *et al.* (CLEO collaboration), Phys. Rev. **D 50**, (1994) 43.
- [29] T. Browder, K. Honscheid, and S. Playfer, in *B decays*, 2nd edition, edited by S. Stone
(World Scientific, Singapore, 1994).
- [30] M. Neubert, V. Rieckert, B. Stech, and Q.P. Xu, in *Heavy Flavours*, edited by A.J.
Buras and H. Lindner (World Scientific, Singapore, 1992).
- [31] A. Deandrea, N. Di Bartolomeo, R. Gatto, and G. Nardulli, Phys. Lett. **B 318**, (1993)
549.
- [32] K. Honscheid, K. Schubert, and R. Waldi, Z. Phys. **C 63**, (1994) 117.
- [33] J.D. Bjorken, Phys. Rev. **D 17**, (1978) 171.
- [34] S.J. Brodsky, C. Peterson, and N. Sakai, Phys. Rev. **D 23**, (1981) 2745.
- [35] C. Peterson, D. Schlatter, J. Schmitt, and P.M. Zerwas, Phys. Rev. **D 27**, (1983) 105.
- [36] J. Chrin, Z. Phys. **C 36**, (1987) 163.
- [37] D. Bortoletto *et al.* (CLEO Collaboration), Phys. Rev. **D 37**, (1988) 1719; Erratum-
ibid. **39** (1989), 1471.

- [38] V. Barger, W.Y. Keung, J.P. Leveille, and R.J.N. Phillips, Phys. Rev. **D 24**, (1981) 2016.
- [39] D.S. Hwang, C.S. Kim, W. Namgung, Preprint SNUTP-95-017 (Feb 95).
- [40] J. Bartelt *et al.* (CLEO Collaboration), Phys. Rev. Lett. **71**, (1993) 4111.
- [41] N. Isgur, D. Scora, B. Grinstein and M.B. Wise, Phys. Rev. **D 39**, (1989) 799.
- [42] I. Bigi, M. Shifman, N.G. Uraltsev, and A. Vainshtein,
Phys. Lett. **B 328**, (1994) 431; Int. J. Mod. Phys. **A 9**, (1994) 2467.
- [43] K. Honscheid, Proceedings of the Rencontres de Moriond 1992, Editions Frontiers.
- [44] H. Albrecht *et al.* (ARGUS Collaboration), Phys. Lett. **B 340**, (1994) 217.
- [45] T.E. Browder and K. Honscheid, Prog. Part. Nucl. Phys. **35**, (1995) 81.

Figure Captions

Fig. 1a Dominant contribution to the decay $B \rightarrow J/\psi X$ with the light final state quark q_f ($f = s, d$) in the subprocess having positive energy.

Fig. 1b Contribution to the decay $B \rightarrow J/\psi X$ with the light final state quark q_f ($f = s, d$) in the subprocess having negative energy.

Fig. 1c $b \rightarrow J/\psi + s(d)$ matrix element. The square represents a four-fermion vertex.

Fig. 2a Momentum (respectively mass) distribution function $f_\varepsilon(x)$ in the IPM for various values of ε_p .

Fig. 2b Mass distribution function $w(x)$ in the ACCMM model for various values of p_f .

- Fig. 3 $x_{\pm}(f = s)$ as functions of the J/ψ momentum for $m_s = 0.125$ GeV (current mass) and for $m_s = 0.55$ GeV (constituent mass).
- Fig. 4 Theoretical momentum spectrum in the IPM for direct inclusive J/ψ production from B decays at the $\Upsilon(4s)$ resonance. The values for the parameters are $m_s = 0.125$ GeV, $m_d = 0$ (current masses), $M_B = 5.279$ GeV, $f_{\psi} = 0.384$ GeV, $|a_2| = 0.275$, $\tau_B = 1.54$ ps, $|V_{cb}| = 0.043$, $|V_{cs}| = 0.97$, $|V_{cd}| = 0.22$ and various values of ε_p as shown.
- Fig. 5 Same as in Fig. 4, now theoretical momentum spectrum for various values of ε_p and $|a_2|$ as shown, compared with the CLEO data.
- Fig. 6 Same as in Fig. 5, now for $\varepsilon_p = 0.008$, $|a_2| = 0.285$ and current, respectively constituent masses for the final state quarks.
- Fig. 7 Theoretical momentum spectrum in the IPM for direct inclusive J/ψ production compared with the corrected CLEO data where the expected contribution of the exclusive two-body final states ($J/\psi K^{(*)}$) has been subtracted. The values for the parameters are $m_s = 0.55$ GeV, $m_d = 0.33$ GeV, $|a_2| = 0.275$ and ε_p as shown.
- Fig. 8 Theoretical momentum spectrum in the ACCMM model for direct inclusive J/ψ production from B decays at the $\Upsilon(4s)$ resonance compared with the CLEO data. The values for the parameters are $m_s = 0.125$ GeV, $m_d = 0$ (current masses), $m_{sp} = 0.2$ GeV, $M_B = 5.279$ GeV, $\tau_B = 1.54$ ps, $|V_{cb}| = 0.043$, $|V_{cs}| = 0.97$, $|V_{cd}| = 0.22$ and various sets of values for p_f and $|a_2|$ as shown.
- Fig. 9 Same as in Fig. 8, now for $p_f = 0.55$ GeV, $|a_2| = 0.28$, $m_{sp} = 0.2$ GeV and current, respectively constituent masses for the final state quarks.
- Fig. 10 Theoretical momentum spectrum for direct inclusive J/ψ production in the ACCMM model for $p_f = 0.55$ GeV, $|a_2| = 0.28$ and various values of m_{sp} as shown compared with the CLEO data.
- Fig. 11 Theoretical momentum spectrum as in Fig. 10, now for $m_{sp} = 0.2$ GeV, $|a_2| = 0.28$ and various values of p_f as shown.

fig. 1a

fig. 1b

fig. 1c

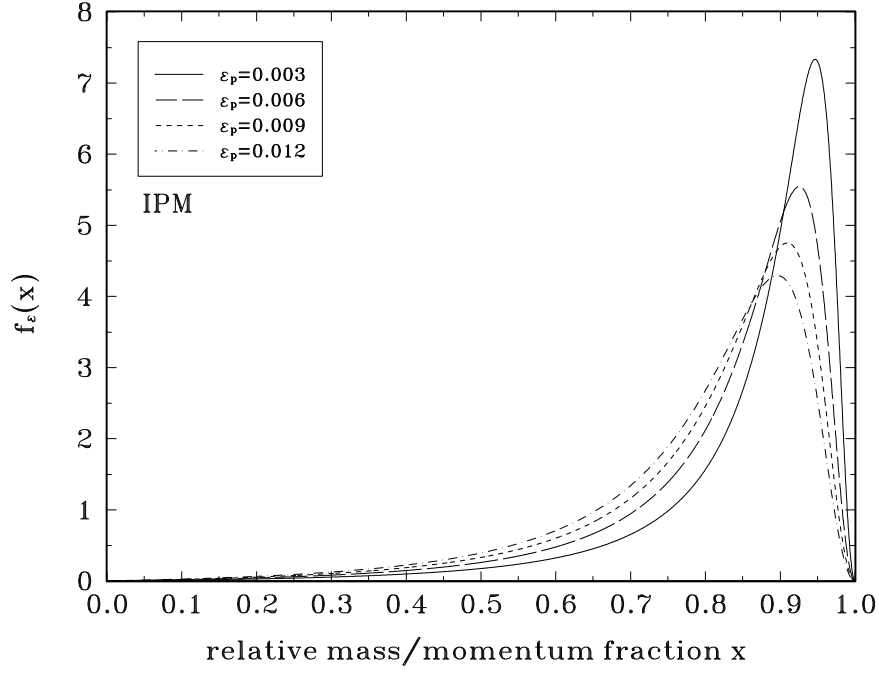


fig. 2a

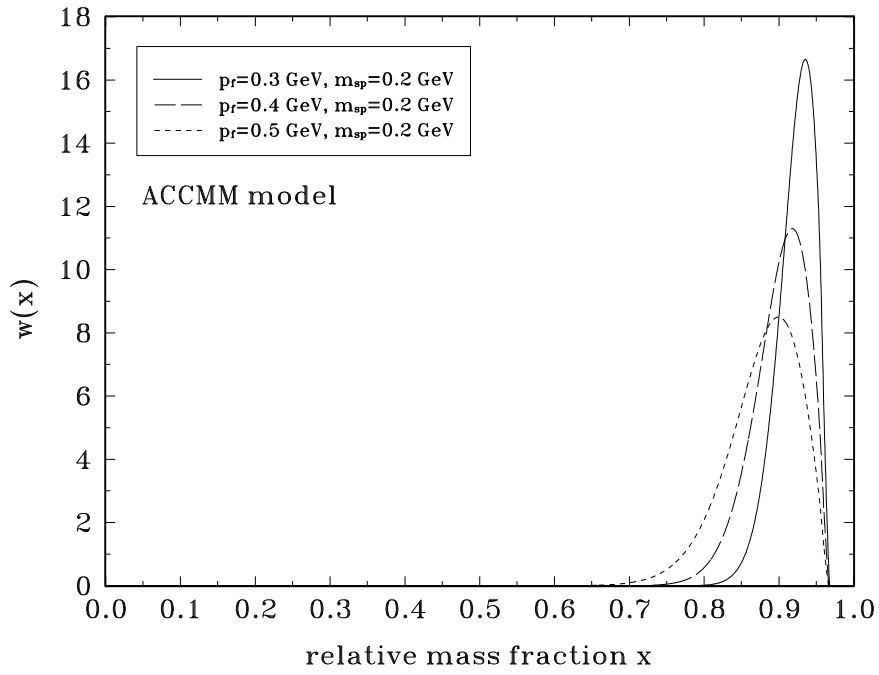


fig. 2b

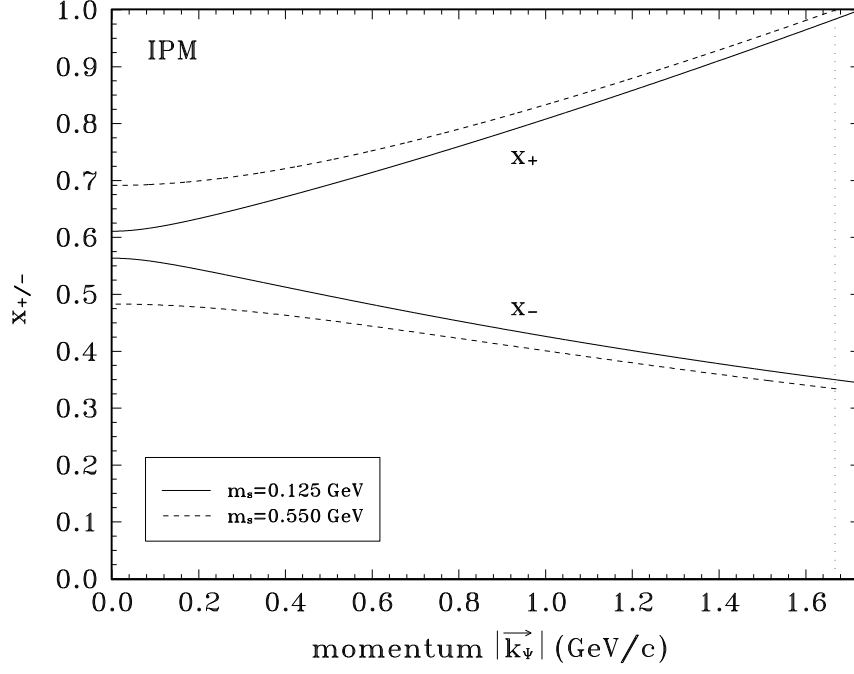


fig. 3

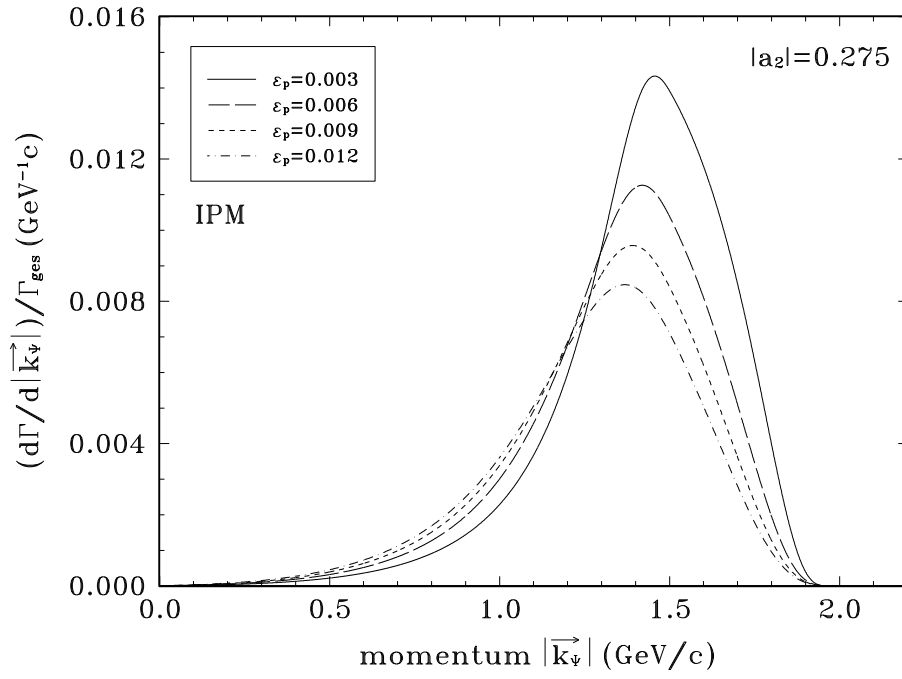


fig. 4

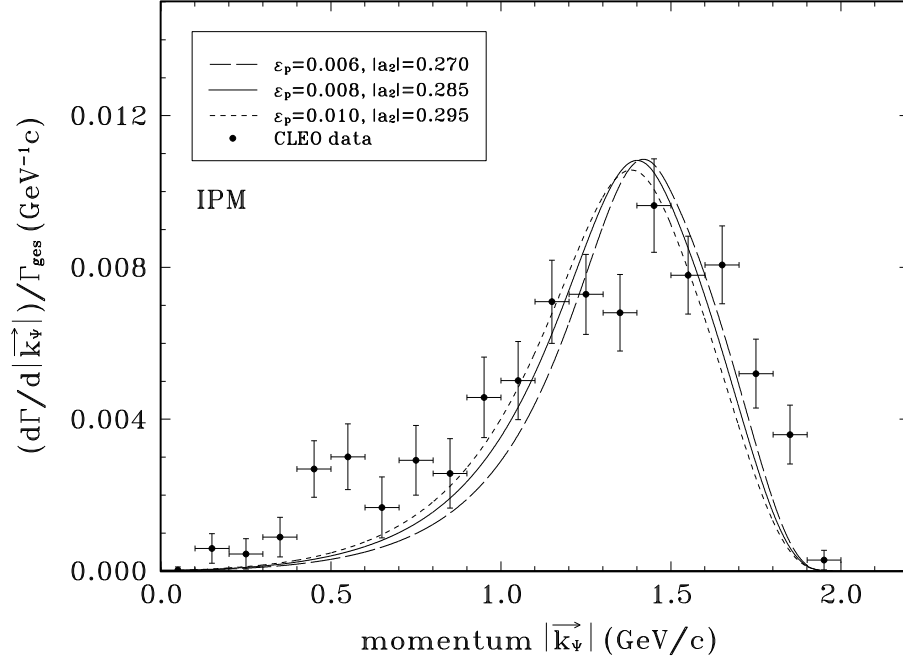


fig. 5

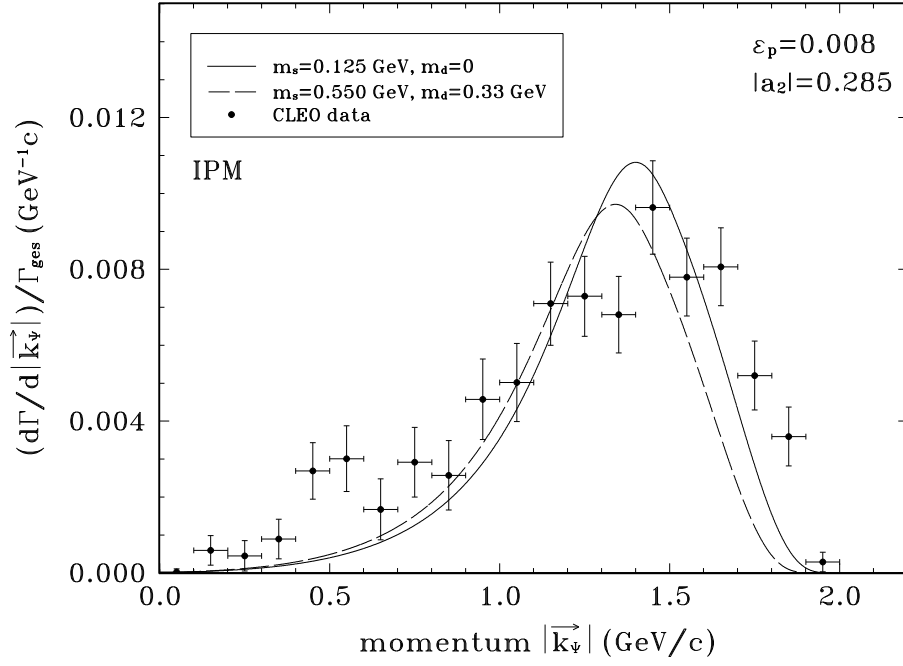


fig. 6

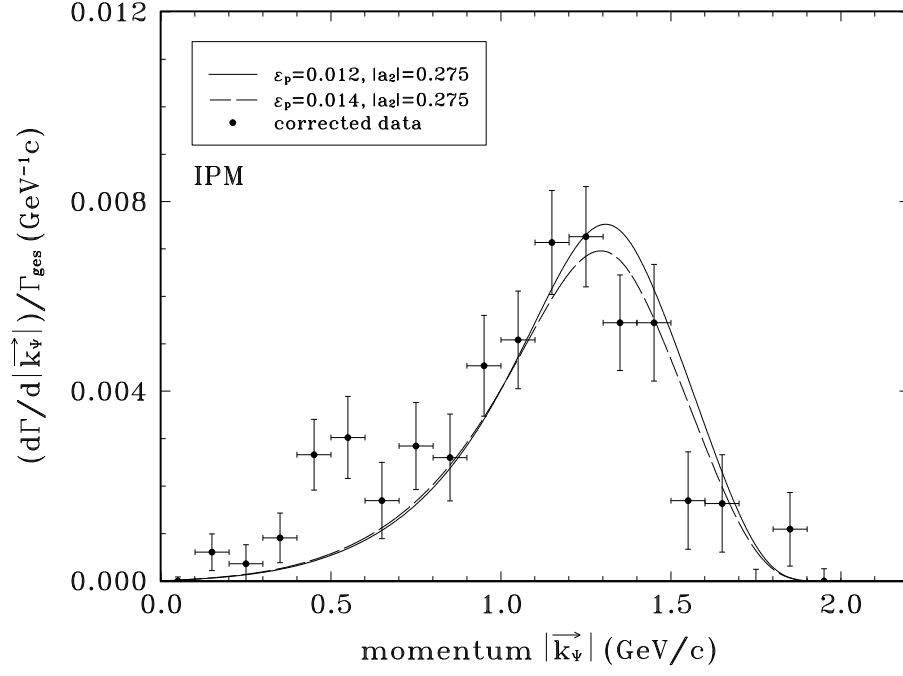


fig. 7

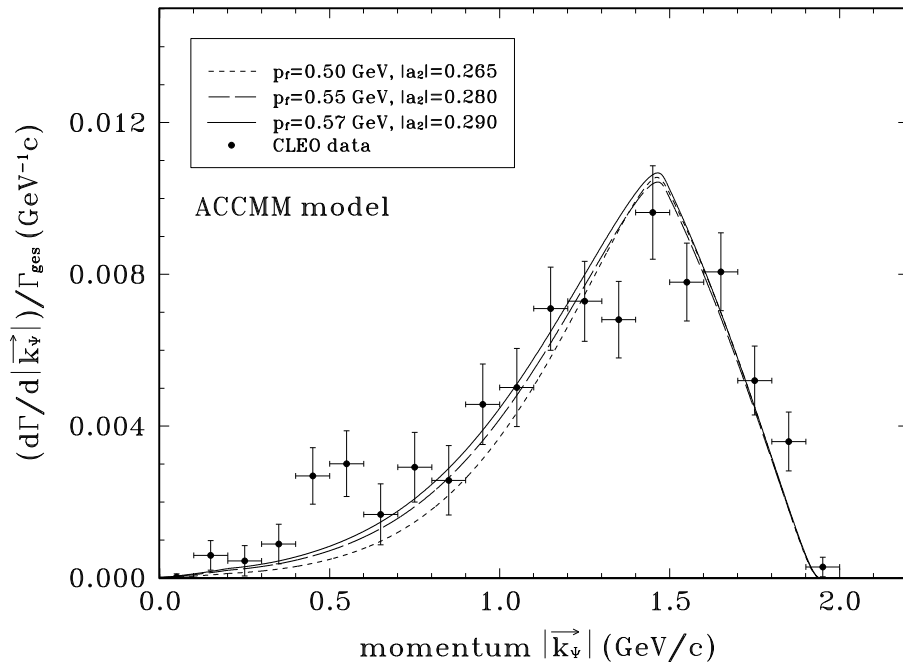


fig. 8

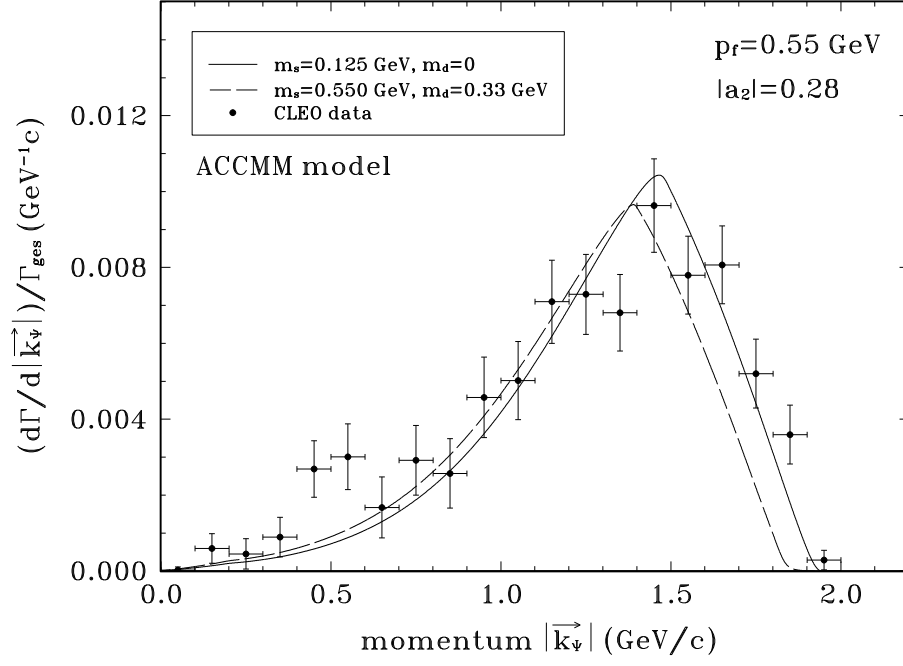


fig. 9

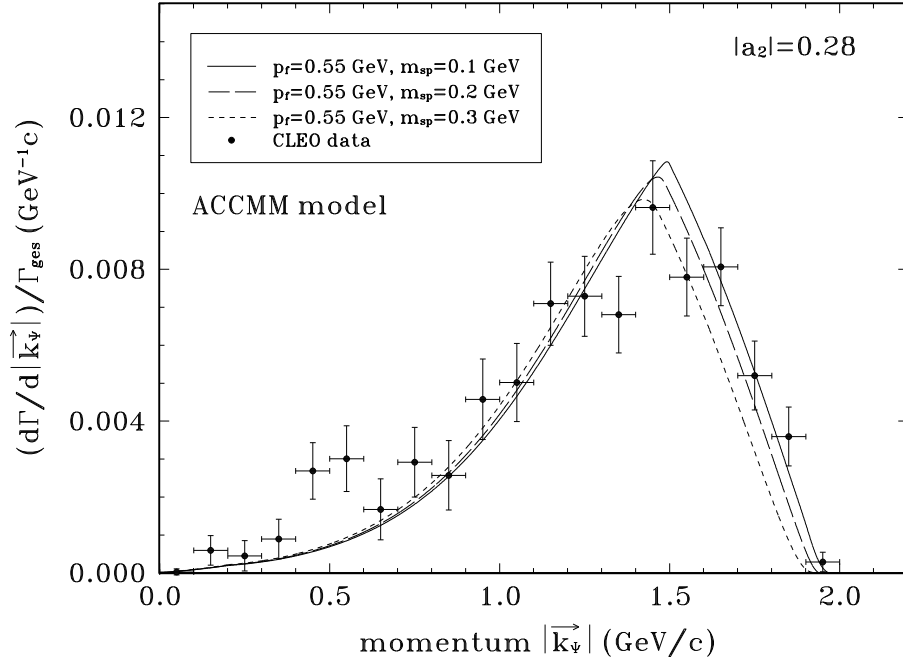


fig. 10

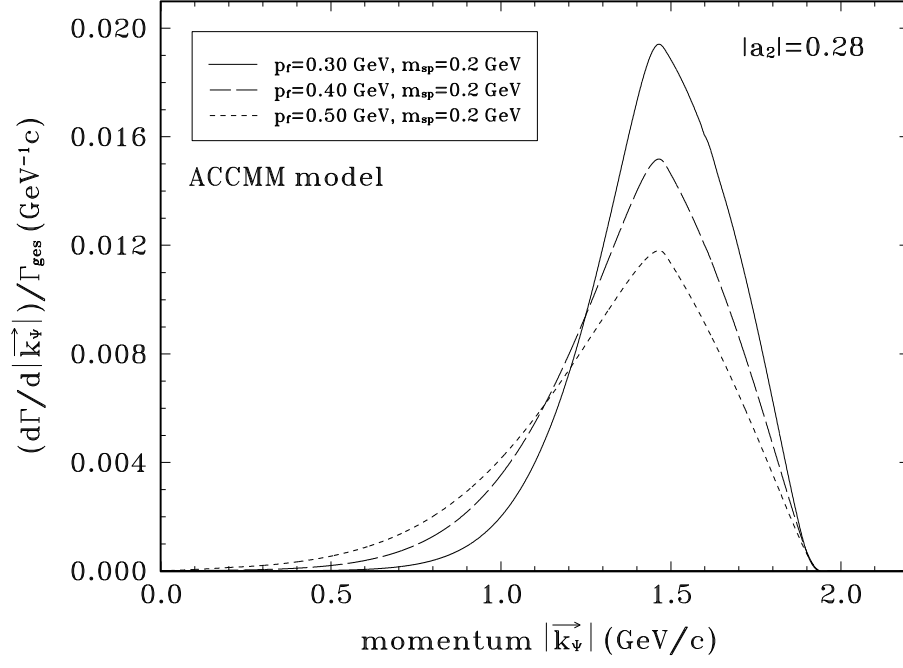


fig. 11